

# STATUS OF HELICAL COOLING CHANNELS FOR INTENSE MUON SOURCES\*

K. Yonehara<sup>†</sup>, Fermilab, Batavia, IL 60510, USA

## Abstract

Status of the design and simulation study of a homogeneously distributed hydrogen gas-filled helical cooling channel (HCC) is presented. The helical cooling theory has been verified by numerical cooling simulations. Flexibility of cooling decrements and equilibrium emittance in the HCC were demonstrated by tuning the helical cooling lattice. Preliminary analysis of a beam-plasma interaction in a solenoid magnetic field and a gas-filled RF cavity was made. As a result, a beam-induced plasma neutralizes a space charge of the incident beam and a plasma-lens effect appears. It indicates that the beam dynamics and cooling performance in the final cooling segment will be affected by the plasma-lens.

## INTRODUCTION

Ionization cooling has a great potential to shrink a muon beam phase space by factor  $10^6$  within their short lifetime ( $2.2\gamma \mu\text{s}$ ) since the collision frequency in a cooling media is extremely high by comparing with a conventional cooling method [1]. However, a large angle scattering takes place by the Coulomb interaction with nuclei in the media, so called a multiple scattering, and grows the muon beam phase space (heating). To minimize the heating, an ionization cooling channel consists of a strong magnetic field to overcome the multiple scattering, and a high-gradient RF cavity in the magnet to immediately compensate the lost-energy via ionization process. Hydrogen is the best cooling material since it has a high energy-loss rate and a long radiation length.

Early days' designs of a cooling channel have a liquid hydrogen flask and a high gradient vacuum RF cavity in a strong magnetic field. However, soon channel designers realize a critical issue that the maximum available RF gradient is strongly limited by the magnetic field strength in the cavity [2]. One plausible model is that dark current densities in the cavity are increased due to focused by magnetic fields. It induces a RF electric breakdown at lower RF gradients in stronger magnetic fields. A possible solution is filling a RF cavity with a dense hydrogen gas [3]. Gas resists the dark current flow and, therefore suppresses RF electric breakdowns even the cavity is operated in a strong magnetic field. In addition, a dense gaseous hydrogen works as an ionization cooling media.

A helical cooling channel (HCC) is designed to maximize the advantage of utilizing the gas-filled RF cavities for a six-dimensional (6D) ionization-cooling channel [4]. Beam trajectory is a spiral by a solenoid and helical mag-

netic components (Fig. 1). To avoid any pressure gap on the beam path, hydrogen gas is distributed homogeneously in the channel. RF cavities are located along the helical beam path without any spatial gap. A thin RF window is located between adjacent cavities to electrically isolate each other. A solenoid and helical dipole components are applied to generate a continuous dispersion. An emittance-exchange occurs during the cooling process with the dispersion, therefore it induces 6D phase space cooling. A helical field gradient continuously focuses the beam and stabilizes the phase space. Large acceptance of the channel is achieved since there is no betatron resonance in the continuous focusing channel. Thus, the channel length is shorter than other ionization cooling channels.

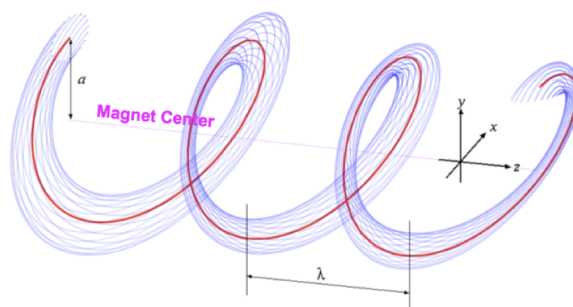


Figure 1: Beam path in a helical lattice. A red line is a reference orbit and a blue line is an orbit of an envelop particle.

Dense hydrogen gas-filled RF cavity is a unique device for beam applications. Particularly, a beam-induced gas-plasma in a dense hydrogen gas opens many interesting subjects. Ionization electrons are quickly thermalized by momentum exchange interaction with molecular hydrogens. The plasma regains kinetic energy from RF fields. The energy is transferred into hydrogen gas via the thermalization. As a result, RF power is transformed into the gas temperature. The rate is proportional to the plasma density in the cavity. It is called plasma loading effect [5]. The effect can be mitigated by doping a small amount of electronegative gas in the cavity. From experiment, 0.2 % Oxygen was sufficient to be ineffective the plasma loading for beam acceleration. Plasma parameters were measured in experiments [6]. These are used in a numerical plasma simulation to evaluate the collective effect in the cavity for intense muon beam applications. As a result, the space charge of beam is neutralized by plasma motions excited by the space charge fields and the tail of the bunched beam is strongly focused by the self-induced axial magnetic field [7, 8]. This phenomenon is similar as the plasma lens that has been developed for the electron-positron collider at SLAC [9]. Since the HCC is a positive energy transition

\* Work supported by Fermilab Research Alliance, LLC under Contract No. DE-AC02-07CH11359

<sup>†</sup> yonehara@fnal.gov

channel the longitudinal space charge force becomes focusing. Therefore, transverse and longitudinal space-charge forces in the HCC will enhance cooling.

Characteristics of the HCC lattice is presented in the first part of document. Then, we discuss about the preliminary study of a gas-plasma dynamics and a beam-plasma interaction in the rest of document.

## DEMONSTRATE COOLING PERFORMANCE IN HCC

### First Cooling Simulation Study

HCC cooling simulation has been done in G4Beamline [10] which has been executed in a parallel grid core processor at NERSC [11]. A solid red line in Fig. 2 shows the simulated emittance evolution in the HCC. An initial cooling channel (a gas-filled helical FOFO, HFOFO snake channel [12]) is applied (a red dash line in Fig. 2) to shrink the initial beam phase space from 15 mm and 45 mm to 4 mm and 7 mm in the transverse and longitudinal phase spaces, respectively.

A matching-in channel is located downstream of the HFOFO to adapt the beam into the HCC with energy transition jump because the HFOFO has a negative energy transition [13]. Current best transmission efficiency is 80 %. The HCC shrinks the 6D beam phase space further. RF frequency is shifted from 325 MHz to 650 MHz in the HCC when the longitudinal beam size becomes small enough to be captured in a high frequency RF bucket. It permits to design a smaller-bore helical magnets that can generate stronger magnetic fields. There are four helical lattice configurations in the first simulation study: The first two HCC segments ( $f = 325$  MHz, helical period  $\lambda = 1.0, 0.8$  m) are designed to have a large acceptance while the last two segments ( $f = 650$  MHz,  $\lambda = 0.5, 0.4$  m) have strong magnetic fields to reach low equilibrium emittances. Helical magnetic field is presented by using analytical field formulae in this simulation [14].

The first cooling cycle in the HCC starts from segment 2. The beam has 21 bunches in this cycle. The bunched beam is merged into one in a low energy helical bunch merge channel to increase beam luminosity [15]. Since the beam size after merge becomes large the second cooling cycle is resumed which will be started from the HCC segment 1. Final emittance is 0.62 mm and 0.88 mm in the transverse and longitudinal planes, respectively. Total channel length and the transmission efficiency including with the matching in the first cooling cycle are 300 m and 48 %, respectively. The HCC theory predicts the equilibrium emittance accurately, 0.62 mm and 0.87 mm in transverse and longitudinal planes, respectively. The prediction agrees quite well with the simulation result.

Table 1 shows the summary of beam parameters and cooling lattice from the design and simulation study. The second cooling cycle has not been accomplished yet since the beam after the bunch merge channel is not ready. Beam growth by mismatching occurs at beginning of each segment. Some amount of particles ( $\sim 5$  %) are lost by mismatching. This

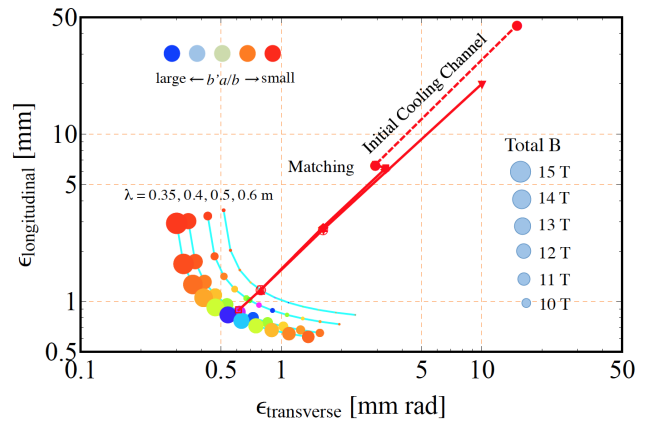


Figure 2: Simulated emittance evolution in the HCC. A light-blue line is the theoretical limit of cooling with various helical periods.

can be eliminated by using more segmented HCCs to make smooth transition.

Table 1: Beam parameters in the HCC. Segment 0 is the initial cooling channel.  $\beta_T$  and  $\beta_L$  are beta functions in transverse and longitudinal planes, respectively. “Tran” is a transmission efficiency at each segment. Segment 4’ is the proposed longitudinal enhance cooling channel.

| Seg | L     | $\lambda$ | $\beta_T$ | $\beta_L$ | $\epsilon_t$ | $\epsilon_l$ | Tran |
|-----|-------|-----------|-----------|-----------|--------------|--------------|------|
|     | m     | m         | cm        | m         | mm           | mm           |      |
| 0   | 100   | –         | 60        | –         | 4.2          | 7.2          | 0.68 |
| 1   | (100) | 1.0       | 20        | 2.1       | –            | –            | –    |
| 2   | 100   | 0.8       | 16        | 2.1       | 1.5          | 2.5          | 0.83 |
| 3   | 120   | 0.5       | 9.8       | 1.5       | 0.75         | 1.2          | 0.82 |
| 4   | 80    | 0.4       | 7.9       | 1.5       | 0.62         | 0.89         | 0.88 |
| 4’  | –     | 0.35      | 7.3       | 1.3       | 0.75         | 0.72         | –    |

### Critical Beam Element Parameter for Cooling Simulation

Figure 3 shows a schematic drawing of the segmented HCC per one helical period. Critical beam parameter is determined from the technological boundary. A magnetron is considered as a RF source that has been developed for accelerator applications [16, 17]. Energy efficiency of a magnetron is extremely high. If the magnetron becomes practical the peak RF power  $\sim 1$  MW will be available. This may be sufficient to excite each high-Q cavity. To this end, the cavity will be operated at 80 K. The peak RF gradient is set to 20 MV/m from the RF power limitation. The estimated RF power deposition in the cavity is less than 0.5 kW/m. A commercial liquid nitrogen chiller is available which has enough cooling power to remove the deposition heat from cavities.

Since the HCC is a positive phase slip factor the RF accelerating phase is set  $\sim 160$  degrees, which generates reasonable longitudinal focusing and cooling rate. The average energy loss rate is  $\sim 6$  MeV/m ( $\sim 10$  MeV per unit channel

length). It determines the hydrogen gas density  $13.4 \text{ mg/cm}^3$ , which corresponds to the gas pressure 160 atm at room temperature (44 atm at 80 K). The cavity length is 10 and 5 cm for 325 and 650 MHz, respectively. In order to make a room in radial direction between RF cavities and helical magnetic coils, a dielectric loaded gas-filled RF cavity has been considered. Proof of principle test of the dielectric loaded RF cavity was made [18]. The radial size of cavity can be reduced by 20 ~ 50 %. A helical re-entrant cavity has also been considered as the option [19].

A 60- $\mu\text{m}$ -thick Beryllium foil is used for a RF window in the cooling simulation. Since hydrogen gas acts as a coolant the frequency detuning due to thermal expansion of the window is negligible. On the other hand, the RF window shape should be curved to avoid the Lorentz force detuning. However, emittance is grown even in the thin RF window. Besides, a small amount of Oxygen dopant which is applied in the cavity also increases the equilibrium emittance. An effective radiation length is given  $X_{0,eff}^{-1} = X_{0,GH_2}^{-1} + X_{0,Be}^{-1} + X_{0,O_2}^{-1}$ . Impurity materials change the equilibrium longitudinal emittance by additional energy loss rates. Modified energy loss rate is applied in the HCC theory to evaluate the longitudinal equilibrium emittance. The effective radiation length model agrees with the numerical simulation although larger discrepancy is seen in thicker RF window.

Helical solenoid coil is innovated to generate proper helical magnetic fields. Solenoid and helical dipole components are naturally generated by superimposing between a main and end (fringe) fields. A helical field gradient is tuned by the coil geometry. A straight solenoid is used to correct the solenoid component. In the magnet design study, the HCC with  $\lambda = 0.5 \text{ m}$  seems to be feasible since the total magnetic field is less than 10 Tesla. However, the last segment,  $\lambda = 0.4 \text{ m}$  is extremely challenging. The total magnetic field

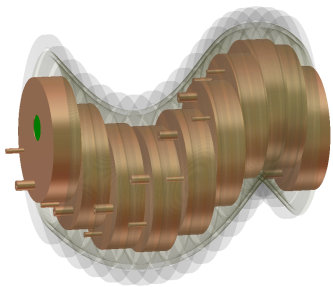


Figure 3: Design concept of the HCC segment. A brown disk is the gas-filled RF cavity which is located on the helical beam path. Each cavity has a power inlet line and a probe. A green surface on the cavity is the RF beam entrance window which is made of a 60- $\mu\text{m}$ -thick Be foil. A gray transparent ring outside the cavity is a helical solenoid coil, which generates proper helical magnetic component. There is a pressure wall between the helical solenoid coils and the RF cavities. Gas sealing and high-pressure feedthrough have been developed in the high-pressure RF experiments.

becomes ~11 Tesla on the helical beam path. Besides, the field on the coil is ~17 Tesla that reaches to the maximum available field strength for  $\text{Nb}_3\text{Sn}$ . Table 2 shows the summary of helical lattice parameters. Huge stored magnetic energy is estimated in last two segments which is generated by the correction solenoid.

Table 2: Cooling lattice parameters in the HCC.  $b$ ,  $b'$ , and  $b_z$  are the helical dipole, field gradient, and solenoid components on a reference orbit, respectively. Segment 4' corresponds to the proposed longitudinal enhance cooling channel instead of using Segment 4. Peak RF power was estimated for the  $\text{Al}_2\text{O}_3$  ceramic loaded RF cavity operating at 80 K.

| Seg. | $b$<br>T | $b'$<br>T/m | $b_z$<br>T | peak RF<br>MW/cavity | Stored B<br>MJ/m |
|------|----------|-------------|------------|----------------------|------------------|
| 1    | 1.24     | -0.21       | 4.2        | 1.1                  | 4.5              |
| 2    | 1.56     | -0.32       | 5.3        | 1.1                  | 4.7              |
| 3    | 2.49     | -0.83       | 8.5        | 0.6                  | 10.7             |
| 4    | 3.11     | -1.29       | 10.6       | 0.6                  | 10.5             |
| 4'   | 3.09     | 5.17        | 11.6       | 0.6                  | -                |

### Reconfigure Cooling Path

It is harder to generate a negative helical field gradient for shorter helical period channel to realize the equal cooling decrements [20]. Adding correction coils and using an elliptic helical solenoid coil have been considered [21]. Here, we discuss another approaches that the helical cooling lattice is reconfigured to mitigate the magnetic field constraint. According to the HCC theory, the longitudinal phase space cooling can be enhanced with smaller dispersion factor, which requires lower helical dipole component than the equal cooling decrements. As a result, a short helical period may be feasible, 0.35 m in the longitudinal enhance cooling. Circles in Fig. 2 shows the predicted achievable equilibrium emittance with various helical periods at various dispersion factors. An emittance which is above (below) a red solid line is generated with larger (smaller) dispersion factor than the factor for the equal cooling decrements. It predicts 0.75 mm and 0.72 mm in the transverse and longitudinal emittances with the magnetic field 12 Tesla (see segment 4' in Tables 1 and 2). Especially, the required helical field gradient is positive for the longitudinal enhance cooling lattice. It significantly mitigates constraint of the helical magnet design and the strength of correction solenoid may be significantly low. This is more plausible solution of the HCC design to achieve lower equilibrium 6D emittance than the original one. We note that the admittance becomes small with a small dispersion factor. Therefore, the dispersion factor should be modulated in the final cooling.

### STUDY BEAM-PLASMA INTERACTION

Gas-filled RF cavity is a unique accelerator device. Three different matters, high energy charged particles, a dense neutral gas, and a beam-induced gas-plasma, exist in the cavity (Figure 4). Ionization process is well-known theoretically

and experimentally. Since gas density is nine-orders of magnitude higher than the density of incident beam no collective effect is concerned in the ionization process. On the other hand, interactions between plasma and dense gas, so called plasma chemistry, is a complicated subject. Hydrogen ions are immediately formed to a hydrogen cluster with molecular hydrogens, i.e.  $H_n^+$  ( $n = 3, 5, 7, \dots$ ). They have different hydrogen neutralization rates and mobilities. Mobilities of electrons strongly depends on a density of hydrogen due to a quantum effect, i.e. the cross-section of Coulomb scattering becomes large when the de Broglie wavelength of thermal electrons is comparable with an average inter distance among molecular hydrogens. Electron capture rate of  $O_2$  dopant is strongly dependent on the density of  $H_2$  since the process occurs as a three-body reaction. Fortunately, overall reactions of the plasma chemistry and plasma processing in a dense gas can be measured in experiments even we do not know the branching ratio for each reaction [6]. The observed values were tested with numerical simulations [8] in which the electron dynamics is described as simple kinematics of electron conduction in a matter.

However, the third interaction, a beam-plasma interaction, cannot be characterized by experiment since there is no accelerator facility to produce  $10^{12} \text{ cm}^{-3}$  beam in nuclear kinetic energies and inject it into a gas-filled RF cavity. We investigated the beam-plasma interaction in numerical simulation. Plasma process is modeled from experimental results. Ionization electrons is quickly thermalized, within a few tens pico seconds, by interacting with a neutral gas. The drift velocity of electrons can be presented by a simple formula,  $v_d = \mu E$ , where  $\mu$  is the mobility of electrons in a gas and  $E$  is a superimposed electric field between the external RF field and the space charge of incident beam. The drift velocity is order of  $10^4 \text{ m/s}$  that is much slower than the

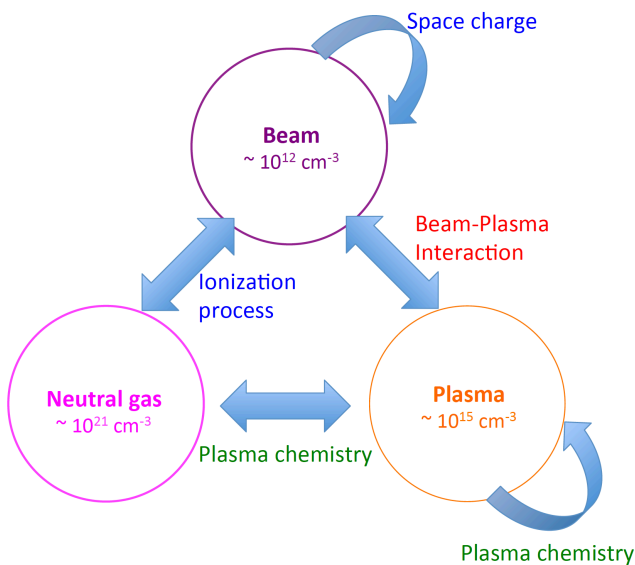


Figure 4: Three states in a gas-filled RF cavity with intense muon beam. Density in each matter is estimated for a muon collider cooling channel.

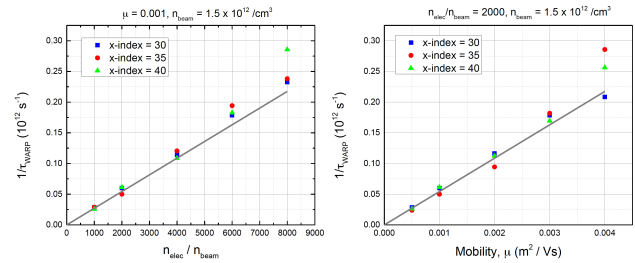


Figure 5: Estimated time constant for the space charge neutralization in the gas-filled RF cavity. Index in plot is the radial distance from the cavity center, i.e. x-index=40 is the cavity center and x-index=30 is the radius of beam.

velocity of an incident beam. However, the density of ionization electrons are three orders of magnitude larger than the incident beam. A density fraction of electrons changes the net electric field strength in the beam volume. If charge of incident muons is negative (positive), electrons are pushed out (in) from the beam volume until net electric fields which is generated by the incident beam and residual positive ions in the beam volume becomes neutral. It is called space charge neutralization.

Time constant of the space charge neutralization is estimated by using a simple formula,  $\tau = \epsilon_0 / (n_e/n_b) \mu E$  and compared to a numerical simulation. Figure 5 shows the estimated time constant of space charge neutralization in analytical and numerical investigations. In this simulation, the plasma was pre-formed before beam injection and plasma and beam densities were uniform. Estimated time constant is  $\sim 20 \text{ ps}$  which is much shorter than the bunch length,  $100 \text{ ps}$ . When the space charge is neutralized the self-induced axial magnetic field becomes dominant and the plasma lens appears.

The plasma lens effect has been studied with a preliminary beam-plasma interaction model. The front end particles generates the plasma, it neutralizes the tailed beam, then the beam is focused by the self-induced axial magnetic field. Envelop equation with the plasma lens is given,

$$\frac{d^2 r_b}{dz^2} + \left( \kappa_{sf} + \frac{\alpha K_b}{r_b^2} \right) r_b = \frac{\epsilon_{KV}^2}{r_b^3}, \quad (1)$$

$$\alpha = \frac{[\beta^2(1 - f_m) - (1 - f_q)]}{1 - \beta^2}, \quad (2)$$

$$K_b = \frac{2r_e}{\gamma^3 \beta^2} \frac{N}{\sqrt{2\pi}\sigma_z}, \quad (3)$$

where  $r_b$  is the radius of beam,  $\kappa_{sf}$  is a focusing strength of a beam lattice,  $K_b$  is a strength of electromagnetic force by the beam,  $\alpha$  is a form factor of the plasma lens.  $f_m$  and  $f_q$  in  $\alpha$  present the fraction of magnetic and electric charges of neutralization plasma.  $\alpha = -1$  corresponds to a pure space charge condition where  $f_m = f_q = 0$ , while  $\alpha = \gamma^2 \beta^2$  is in the complete space charge neutralization where  $f_m = 0, f_q = 1$ . The focusing force is  $\gamma^2 \beta^2$  larger than the space charge force. Therefore, even the space charge

is not affected on the beam dynamics the plasma lens can show up and influence on the beam dynamics. Figure 6 shows the result of plasma lens in numerical simulation by using WARP [22].

The plasma focusing force is stronger with smaller phase space beam. There is no theoretical limit on the plasma focusing until the beam size reaches to the quantum thermal noise. The process seems to be the new focusing mechanism to have the extremely cold muon beam. Further study is required.

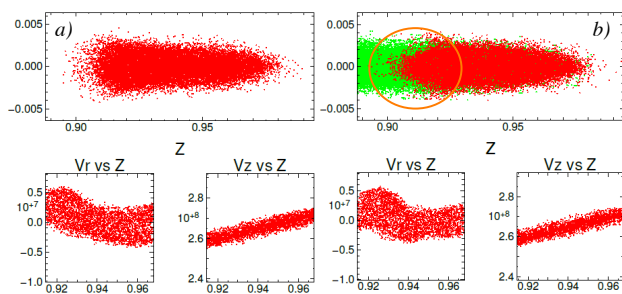


Figure 6: WARP simulation shows the plasma lens effect without gas (a) and with gas (b). Only a straight solenoidal magnetic field and RF fields are applied, but no dispersion in this simulation. Orange circle shows that the beam is focused by the plasma lens.

## ACKNOWLEDGMENT

Author thanks to the helical cooling channel design and simulation group. Author also thanks to MAP and Muons, Inc. for great supporting the design efforts and the machine developments.

## REFERENCES

- [1] D. Neuffer, *Particle Accelerators* **14** (1983) 75.; A.N. Skrinsky and V.V. Parkhomchuk, *J. Nucl. Physics* **12** (1981) 3.; D. Neuffer, "Introduction to Muon Cooling", *Nucl. Inst. and Meth.* **A532** (2004) 26.
- [2] A. Moretti et al., "Effects of high solenoidal magnetic fields on rf accelerating cavities", *Phys. Rev. STAB* **8** (2005) 072001.
- [3] R.P. Johnson et al., "High Pressure, High Gradient RF Cavities for Muon Beam Cooling", *Proc. of LINAC2004* (2004) 266.; P. Hanlet et al., "High Pressure RF Cavities in Magnetic Fields", *Proc. of EPAC2006* (2006) 1364.
- [4] Y.S. Derbenev and R.P. Johnson, "Six-dimensional muon beam cooling using a homogeneous absorber; Concepts,

beam dynamics, cooling decrements, and equilibrium emittances in a helical dipole channel", *Phys. Rev. STAB* **8** (2005) 041002.

- [5] M. Chung et al., "Pressurized  $H_2$  rf Cavities in Ionizing Beams and Magnetic Fields", *Phys. Rev. Lett.* **111** (2013) 184802.
- [6] B. Freemire et al., "Pressurized RF Cavities in Ionizing Beams", Submitted to *Phys. Rev. STAB*.
- [7] J. Ellison et al., "Beam-plasma Effects in Muon Ionization Cooling Lattices", *Proc. of IPAC2015* (2015) 2649.
- [8] K. Yu et al., "SPACE code for Beam-plasma Interaction", *Proc. of IPAC2015* (2015) 728.; K. Yu et al., "Simulation of beam-induced plasma in a gas-filled RF cavity", Submitted to JINST.
- [9] T. Katsouleas et al., "Plasma physics at the final focus of high-energy colliders", *Phys. of Fluids* **B2** (1990) 1384.
- [10] G4beamline, <http://public.muonsinc.com/Projects/G4beamline.aspx>
- [11] NERSC, <https://www.nersc.gov/>.
- [12] Y. Alexahin, "Helical FOFO Snake for Initial 6D Cooling of Muons", *ICFA Beam Dyn. Newslett.* **65** (2014) 49.
- [13] C. Yoshikawa et al., "Design and Simulation of A Matching System into the Helical Cooling Channel", *Proc. of IPAC2014* (2014) 1382.
- [14] T. Tominaka et al., "Analytical Field Calculation of Helical Coils", *Nucl. Instr. Meth.* **A459** (2001) 398.
- [15] A. Sy et al., "Matching into the Helical Bunch Coalescing Channel for a High Luminosity Muon Collider", *Proc. of IPAC2015* (2015) 2315.
- [16] G. Kazakevich et al., "High-power Magnetron Transmitter as an RF Source for Superconducting Linear Accelerators", *Nucl. Instr. Meth.* **A760** (2014) 19.
- [17] B. Chase et al., "Precision Vector Control of a Superconducting RF Cavity Driven by an Injection Locked Magnetron", *JINST arXiv:1502.04118v1* (2014).
- [18] L.M. Nash et al., "High Power Tests of Alumina in High Pressure RF Cavities for Muon Ionization Cooling Channel", *Proc. of IPAC2013* (2013) 1508.; B. Freemire et al., "Low Powered RF Measurements of Dielectric Materials for use in High Pressure Gas Filled RF Cavities", *Proc. of IPAC2015* (2015) 3387.
- [19] F. Marhauser et al., "RF Cavity Design Aspects for a Helical Muon Beam Cooling Channel", *Proc. of IPAC2014* (2014) 3352.
- [20] M. Lopes et al., "Magnetic Design Constraints of Helical Solenoids", *Proc. of IPAC2014* (2014) 2731.
- [21] S.T. Krave et al., "A Concept for a High-Field Helical Solenoid", *Proc. of IPAC2015* (2015) 3345.; S. Kahn et al., "Conceptual Design of the Muon Cooling Channel to Incorporate RF Cavities", *Proc. of IPAC2014* (2014) 1325.; M.L. Lopes et al., "Alternate Methods for Field Corrections in Helical Solenoids", *Proc. of IPAC2015* (2015) 3409.
- [22] WARP, [http://blast.lbl.gov/BLASTcodes\\_Warp.html](http://blast.lbl.gov/BLASTcodes_Warp.html).